Supplemental material: Enhanced quantum oscillatory magnetization and non-equilibrium currents in an interacting two-dimensional electron system in MgZnO/ZnO with repulsive scatterers

M. Brasse,[1] S. M. Sauther,[1] J. Falson,[2] Y. Kozuka,[2] A. Tsukazaki,[3]
Ch. Heyn,[4] M. A. Wilde,[1,*] M. Kawasaki,[2] and D. Grundler[1]

[1]*Lehrstuhl für Physik funktionaler Schichtsysteme, Technische Universität München, 85748 Garching, Germany*
[2]*Department of Applied Physics and Quantum-Phase Electronics Center (QPEC), University of Tokyo, Tokyo 113-8656, Japan*
[3]*Institute for Materials Research, Tohoku University, Sendai 980-8577, Japan, and PRESTO, Japan Science and Technology Agency (JST), Tokyo 102-0075, Japan*
[4]*Institut für Angewandte Physik, Universität Hamburg, Jungiusstrasse 11, 20355 Hamburg, Germany*

(Dated: January 8, 2014)

I. SAMPLE DETAILS

The heterostructure was grown using molecular beam epitaxy with high-purity 7 N Zn and 6 N Mg metals as well as distilled pure ozone as the oxygen source. The heterostructure was formed by depositing a 690 nm-thick ZnO layer followed by a 380 nm-thick MgZnO layer on a Zn-polar ZnO substrate. A 2DES is spontaneously formed at the interface without remote doping of donors due to the polarization mismatch between the ZnO and MgZnO layers. To allow for cantilever magnetometry experiments, the sample was cut by a wiresaw and polished from the backside to reduce the thickness of the substrate to about 30 μm. The sample/2DES area amounts to $A = 0.9 \times 1.8$ mm^2
The micromechanical cantilever was prepared from an undoped AlGaAs/GaAs heterostructure grown by molecular-beam epitaxy using optical lithography and sophisticated wet chemical etching techniques[1]. The sample was glued to the flexible end of the cantilever beam using high vacuum grease. Figure 1 shows a photograph of a thinned MgZnO/ZnO sample attached to a GaAs-based micromechanical cantilever magnetometer. The cantilever is glued to an Au-coated sapphire substrate containing the contact pads and guard plane for the capacitive readout[2].

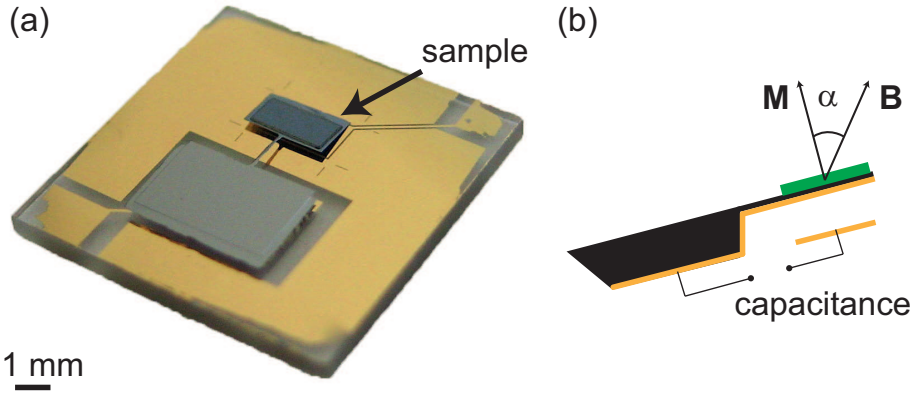

FIG. 1: (a) Photo of a thinned MgZnO/ZnO sample on micromechanical cantilever sensor. The cantilever was prepared from an undoped AlGaAs/GaAs heterostructure. The active MgZnO/ZnO 2DES area is 1.8×0.9 mm^2. (b) Schematic side-view of the measurement setup.

II. TRANSPORT CHARACTERIZATION

Transport experiments have been conducted on a reference sample cut from the same heterostructure at $T = 0.5$ K using the van-der-Pauw method. We refer to this sample as reference sample A in the following. The results for R_{xx} (blue line) and R_{xy} (red line) are shown in Fig. 2. Analyzing the Shubnikov-de Haas oscillations and the Hall effect

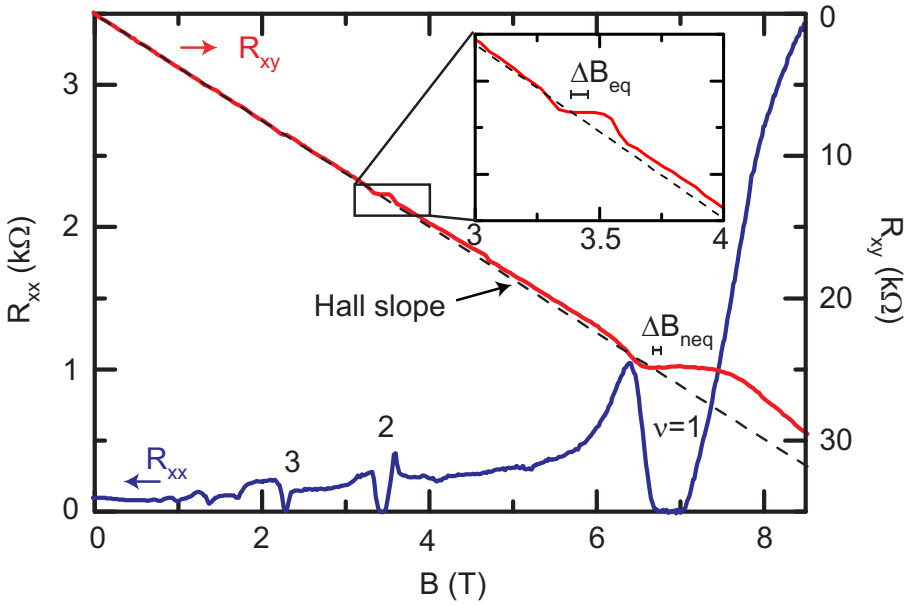

FIG. 2: Transport characterization of the MgZnO/ZnO reference sample A at $T = 0.5$ K yields $n_s = 1.7 \times 10^{11}$ cm^{-2} and $\mu = 3.8 \times 10^5$ cm^2/Vs. The crossing of the Hall slope with the Hall plateaus at $\nu = 1$ and $\nu = 2$ does not occur in the center of the respective plateau. Instead, the plateaus as well as the R_{xx} minima are shifted to larger fields. The shifts ΔB_{neq} and ΔB_{eq} observed in the magnetometry experiment are indicated.

yields $n_s = 1.7 \times 10^{11}$ cm^{-2} and $\mu = 3.8 \times 10^5$ cm^2/Vs. The classical Hall slope extrapolated from the low field data is shown by the dashed line. At $\nu = 2$ and $\nu = 1$, the Hall plateaus in R_{xy} do not occur symmetrically with respect to the classical Hall slope. Instead, the Hall plateaus as well as the R_{xx} minima are shifted to larger fields. Following Refs. 3–5, this behavior is attributed to the presence of repulsive scatterers being in close vicinity to the 2DES.

III. MAGNETIZATION OF A REFERENCE 2DES

In order to establish whether the observed magnetization features occur systematically, additional magnetization experiments were conducted, following the measurement procedure described in the main text. Here, a second 2DES sample cut from the same heterostructure was used, which we will refer to as reference sample B in the following. The result of the experiment at $T = 0.28$ K and $\alpha = 52°$ is depicted in Fig. 3. The jumps in the magnetization at $\nu = 2$ and $\nu = 1$ can be ascribed to the dHvA effect. A signal stemming from the NECs, which changes sign upon changing sweep direction, is present at $\nu = 1$. The behavior as a function of temperature of both, dHvA effect and NECs, is consistent with the one described in the main text (not shown). The NEC maxima at $\nu = 1$ and the position of the dHvA oscillation at $\nu = 2$ shift systematically towards lower fields with increasing temperature. In comparison to the results shown in the main text, the observed signal amplitudes of the dHvA effect and the NECs are smaller here. Regarding the dHvA effect, we observe $\Delta M_{e,\nu=2} = 0.6\ \mu_B^*$ and $\Delta M_{e,\nu=1} = 0.8\ \mu_B^*$. These values are by a factor of 2 to 3 smaller than the ones reported in the main text. The dHvA effect at $\nu = 3$ was not resolved. The signal arising from the non-equilibrium magnetization M_{NEC} is reduced by a factor of 10.

The reduced signal amplitudes in the reference sample B might be ascribed to variations in the 2DES homogeneity and mobility within the MgZnO/ZnO heterostructure such that the 2DES properties vary more strongly in reference sample B. It is well established that the dHvA effect is very sensitive to disorder and sample inhomogeneity[2,6]. Their mutual effect is to wash out the dHvA oscillations. However, we clearly observe consistent temperature dependent shifts of equilibrium- as well as non-equilibrium magnetization signals on the B-field axis also in the reference sample B, *despite* the apparent differences in the sample parameters. This indicates that the observed phenomena are quite robust.

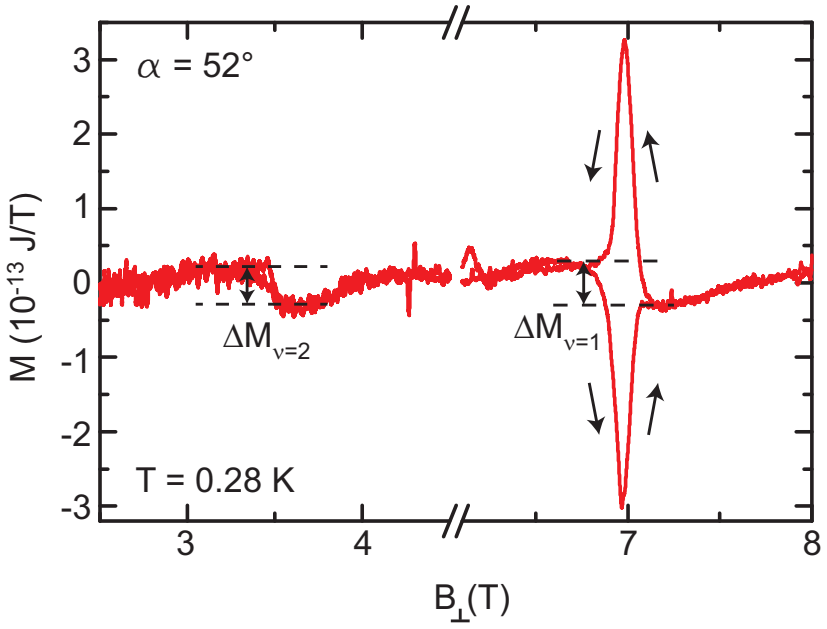

FIG. 3: Magnetization as a function of $B_\perp$ of reference sample B at $T = 0.28$ K and $\alpha = 52°$. At $\nu = 2$ and $\nu = 1$, the data exhibits the dHvA effect. The amplitudes per electrons are $\Delta M_{\mathrm{e},\nu=2} = 0.6\ \mu_{\mathrm{B}}^*$ and $\Delta M_{\mathrm{e},\nu=1} = 0.8\ \mu_{\mathrm{B}}^*$, respectively. NECs are resolved near $\nu = 1$. The amplitude of M_{NEC} amounts to $\sim 3 \times 10^{-13}$ J/T.

IV. MODEL CALCULATIONS

We performed numerical model calculations in the single particle picture following Ref. 2 to analyze the experimental results. In an ideal 2DES the energy spectrum of the 2DES is composed of discrete levels $E_{\mathrm{j,s}} = (j+1/2)\hbar\omega_{\mathrm{c}} + sg\mu_{\mathrm{B}}B$ and the corresponding density-of-states (DOS) is a series of delta-peak shaped Landau levels. Disorder in a real 2DES leads to a broadening of the Landau levels. For this case we model the DOS with a Gaussian line shape given by

$$D(E) = \frac{eB_\perp}{h} \sum_{j=0}^{\infty} \frac{1}{\sqrt{2\pi}\Gamma} \exp\left[\frac{(E - E_{\mathrm{j,s}})^2}{2\Gamma^2}\right]. \tag{1}$$

Here, we take level broadening by $\Gamma = \frac{e\hbar}{m^*}\sqrt{2/\pi\mu}\sqrt{B_\perp}$[7] into account. For the given heterostructure Γ amounts to $5 \times 10^{-2}\sqrt{B_\perp}$ meVT$^{-1/2}$. We further include finite temperature effects via the Fermi-Dirac distribution

$$f(E, \chi, T) = \left[1 + \exp\left(\frac{E - \chi}{k_{\mathrm{B}}T}\right)\right]^{-1}, \tag{2}$$

where χ denotes the chemical potential. χ and the free energy F can then be determined in a self-consistent way from the number of electrons $N = An_{\mathrm{s}}$ via

$$N = A \int f(E, \chi, T) D(E) \mathrm{d}E, \tag{3}$$

$$F = \chi N - k_{\mathrm{B}}TA \int D(E) \ln\left[1 + \exp\left(\frac{\chi - E}{k_{\mathrm{B}}T}\right)\right] \tag{4}$$

This allows us to calculate the thermodynamic equilibrium quantity M given by

$$M = -\partial F/\partial B|_{T,n_{\mathrm{s}}} \tag{5}$$

and to model $M(B_\perp)$ as depicted in the inset of Fig. 1 in the main text.

---

* mwilde@ph.tum.de

[1] M. P. Schwarz, D. Grundler, I. Meinel, C. Heyn, and D. Heitmann, Appl. Phys. Lett. **76**, 3564 (2000).
[2] M. A. Wilde, J. I. Springborn, O. Roesler, N. Ruhe, M. P. Schwarz, D. Heitmann, and D. Grundler, physica status solidi (b) **245**, 344 (2008).
[3] J. E. Furneaux and T. L. Reinecke, Phys. Rev. B **33**, 6897 (1986).
[4] R. J. Haug, R. R. Gerhardts, K. v. Klitzing, and K. Ploog, Phys. Rev. Lett. **59**, 1349 (1987).
[5] A. Raymond, I. Bisotto, Y. M. Meziani, S. Bonifacie, C. Chaubet, A. Cavanna, and J. C. Harmand, Phys. Rev. B **80**, 195316 (2009).
[6] J. P. Eisenstein, H. L. Stormer, V. Narayanamurti, A. Y. Cho, A. C. Gossard, and C. W. Tu, Phys. Rev. Lett. **55**, 875 (1985).
[7] T. Ando and Y. Uemura, J. Phys. Soc. Jpn. **36**, 959 (1974).